Theor Appl Genet (2012) 124:1375–1387
DOI 10.1007/s00122-012-1794-x

ORIGINAL PAPER

An expectation and maximization algorithm for estimating $Q \times E$ interaction effects

Fuping Zhao · Shizhong Xu

Received: 20 June 2011 / Accepted: 5 January 2012 / Published online: 2 February 2012

Abstract A Markov chain Monte Carlo (MCMC) implemented Bayesian method has been developed to detect quantitative trait loci (QTL) effects and $Q \times E$ interaction effects. However, the MCMC algorithm is time consuming due to repeated samplings of QTL parameters. We developed an expectation and maximization (EM) algorithm as an alternative method for detecting QTL and $Q \times E$ interaction. Simulation studies and real data analysis showed that the EM algorithm produced comparable result as the Bayesian method, but with a speed many magnitudes faster than the MCMC algorithm. We used the EM algorithm to analyze a well known barley dataset produced by the North American Barley Genome Mapping Project. The dataset contained eight quantitative traits collected from 150 doubled-haploid (DH) lines evaluated in multiple environments. Each line was genotyped for 495 polymorphic markers. The result showed that all eight traits exhibited QTL main effects and $Q \times E$ interaction effects. On average, the main effects and $Q \times E$ interaction effects contributed 34.56 and 16.23% of the total phenotypic variance, respectively. Furthermore, we found that whether or not a locus shows $Q \times E$ interaction does not depend on the presence of main effect.

Communicated by M. Sillanpaa.

Electronic supplementary material The online version of this article (doi:10.1007/s00122-012-1794-x) contains supplementary material, which is available to authorized users.

F. Zhao · S. Xu (✉)
Department of Botany and Plant Sciences,
University of California, Riverside, CA 92521, USA
e-mail: shizhong.xu@ucr.edu

Introduction

The mixed model methodology (Henderson 1975) offers an efficient tool for detecting $Q \times E$ interaction for complex quantitative traits with the same set of genotypes measured in multiple environments (Piepho 2000). Under the mixed model framework, we can treat some effects as fixed and others as random, depending on the interpretations of the effects and mathematical convenience of the analysis. Piepho (2000) chose quantitative trait loci (QTL) effects as fixed and environmental effects as random. However, the author used a single marker or interval mapping approach to analyzing the QTL effect and $Q \times E$ interaction. The entire experiment requires multiple analyses with one locus at a time. When multiple QTL are included in a single model, a variable selection scheme may be used because the number of markers can be larger than the sample size. Bayesian shrinkage analysis can handle multiple QTL in a convenient way so that variable selection can be avoided (Xu 2003). In the Bayesian shrinkage analysis, a model can handle many more QTL effects than that can be handled by the traditional maximum likelihood method, even if the number of effects is larger than the sample size. The original Bayesian shrinkage method proposed by Xu (2003) has been applied to QTL mapping within one environment. The method has been extended to mapping $Q \times E$ interaction effects by Chen et al. (2010). The method was implemented via the Markov Chain Monte Carlo (MCMC) algorithm. For any particular marker, the mean of the marker effects across multiple environments represented the main effect and the variance of the marker effects across multiple environments represented the $Q \times E$ interaction effect.

The MCMC-implemented Bayesian method generally provides the highest accuracy of QTL effect estimation, but

is computationally very demanding, especially for large models coupled with large sample sizes. To improve the computational efficiency, Xu (2010) proposed a fast expectation and maximization (EM) algorithm to estimate the posterior modes of variance parameters while the regression coefficients were treated as missing values. This algorithm can also capitalize on valuable information on the basis of prior distribution and is always faster than the MCMC-implemented shrinkage analysis. In this study, we extended the EM algorithm of Xu (2010) to multiple environments for detecting QTL main effects and $Q \times E$ interaction effects.

The doubled-haploid barley data published by Hayes et al. (1993) have been analyzed by numerous investigators (Attari et al. 1998; Fang et al. 2008; Han et al. 1995, 1997; Romagosa et al. 1996; Xu and Hu 2010). They are good sample data for $Q \times E$ interactions because the DH lines were evaluated in multiple environments. The DH population was derived from the cross of "Steptoe" and "Morex", where "Steptoe" is the dominant feed barley in the Northwestern US and "Morex" is the six-row Spring US malting quality standard. There were four agronomic traits (Grain yield, Lodging, Heading date and Height) and four malting quality traits (Grain protein, Alpha amylase, Diastatic power and Malt extract) measured in various numbers of environments. A total of 495 markers were genotyped for 150 DH lines with an average marker interval of 2.23 cM. This dataset was previously analyzed by Hayes et al. (1993) using 123 markers with an average marker density of 9.6 cM. The authors took a least squares approach under the interval mapping scheme for detection of QTL and $Q \times E$ interaction effects (Hayes et al. 1993). However, simultaneous analysis of multiple loci under multiple environments has not been conducted for this barley population. The result of multiple QTL and $Q \times E$ effect analysis should be more informative and can be used to direct further experiments and molecular breeding in barley.

Methods

Hierarchical model

The method is developed based on a doubled diploid (DH) design. Let m be the number of environments and n be the number of DH lines. Define $y_j = [y_{j1}\, y_{j2} \cdots y_{jm}]^{\mathrm{T}}$ as an $m \times 1$ vector for the observed phenotypic values of line j measured from the m environments. The linear model for y_j is

$$y_j = \beta + \sum_{k=1}^{q} Z_{jk}\gamma_k + \xi_j \quad (1)$$

where β is an $m \times 1$ vector of intercepts, Z_{jk} is a numerically coded genotypic indicator variable for line j at locus k, for $k = 1, \ldots, q$, where q is the number of markers, $\gamma_k = [\gamma_{k1}\, \gamma_{k2} \cdots \gamma_{km}]^{\mathrm{T}}$ is an $m \times 1$ vector for the regression coefficients of the phenotypic values on the numerically coded genotype. Note that γ_k is a vector and Z_{jk} is a scalar. To model the $Q \times E$ interaction effect, we assume that γ_k follows a multivariate normal distribution given below:

$$p(\gamma_k|\alpha_k, \sigma_k^2) = N(\gamma_k|1_m\alpha_k, I_{m\times m}\sigma_k^2) \quad (2)$$

where 1_m is a unity vector with dimension m, $I_{m\times m}$ is an $m \times m$ identity matrix, α_k is the mean value representing the QTL main effect and σ_k^2 is the variance of m environment-specific QTL effects represented by vector γ_k. This variance represents the $Q \times E$ interaction for locus k. This type of model with a further modeling on γ_k is called the hierarchical model. In the hierarchical model, the first moment parameter α_k is the main effect and the second moment parameter σ_k^2 represents the degree of $Q \times E$ interaction, called the $Q \times E$ interaction effect in this report. In the multivariate model shown in Eq. 1, the residual error vector $\xi_j = [\xi_{j1}\, \xi_{j2} \cdots \xi_{jm}]^{\mathrm{T}}$ is assumed to be multivariate normal denoted by $\xi_j \sim N(0, \Theta)$, where Θ is an $m \times m$ variance–covariance matrix. For simplicity, we chose $\Theta = I_{m\times m}\sigma^2$ as the residual variance–covariance structure, called homogenous residual error variance. Other structures are described in the discussion section.

Prior distribution

We often have enough information from the data to estimate β and σ^2, and thus a uniform prior can be assigned to each of them. The QTL main effect α_k and the $Q \times E$ interaction effect σ_k^2 are the parameters of interest. The main effect for the kth QTL is assigned the following normal prior,

$$p(\alpha_k|\varphi_k^2) = N(\alpha_k|0, \varphi_k^2) \quad (3)$$

where φ_k^2 is the prior variance. Following Xu (2010) and Yi and Xu (2008), we consider two classes of priors for φ_k^2. The first class is the scaled inverse Chi-square distribution assigned to φ_k^2, which is

$$p(\varphi_k^2|\tau_\varphi, \omega_\varphi) = \mathrm{Inv} - \chi^2(\varphi_k^2|\tau_\varphi, \omega_\varphi) \quad (4)$$

A special case of this prior is $(\tau_\varphi, \omega_\varphi) = (-2, 0)$, which is equivalent to the uniform prior $p(\phi_k^2) = 1$. The other special case is $(\tau_\varphi, \omega_\varphi) = (0, 0)$, which represents the Jeffrey's prior, i.e., $p(\varphi_k^2) = 1/\varphi_k^2$. The second class of the priors is the exponential distribution,

$$p(\varphi_k^2|\lambda_\varphi) = \text{Expon}\left(\varphi_k^2|\frac{\lambda_\varphi^2}{2}\right) = \frac{\lambda_\varphi^2}{2}\exp\left(-\frac{\lambda_\varphi^2}{2}\varphi_k^2\right) \quad (5)$$

where λ_φ^2 is the regularization parameter. This exponential prior will result in the Lasso estimation of QTL main effects (Tibshirani 1996), and thus is called the Lasso parameter.

In a similar manner, two different priors are assigned to variance σ_k^2 (representing the $Q \times E$ interaction). The first prior is the scaled inverse Chi-square prior distribution,

$$p(\sigma_k^2|\tau_\sigma, \omega_\sigma) = \text{Inv} - \chi^2(\sigma_k^2|\tau_\sigma, \omega_\sigma) \quad (6)$$

The second prior is the exponential prior,

$$p(\sigma_k^2|\lambda_\sigma) = \text{Expon}\left(\sigma_k^2|\frac{\lambda_\sigma^2}{2}\right) = \frac{\lambda_\sigma^2}{2}\exp\left(-\frac{\lambda_\sigma^2}{2}\sigma_k^2\right) \quad (7)$$

This exponential prior will lead to the Lasso estimations of environment-specific QTL effects. Note that (τ, ω) and λ^2 are hyper-parameters set up by the investigators. For simplicity, we chose the same hyper-parameters for both φ_k^2 and σ_k^2.

Joint posterior

In the Bayesian shrinkage analysis, the inferences of the parameters are made based on the marginal posterior distributions. The MCMC algorithm can obtain the posterior information of the parameters sampled from the posterior distributions. However, the EM algorithm obtains the posterior modes of the parameters by maximizing the joint density of the posterior. This posterior mode estimation is achieved via an iterative algorithm in lieu of a posterior expectation. The posterior distribution is a combination of the prior and the likelihood. Let $\theta = \{\beta, \sigma^2, \alpha_k, \gamma_k, \varphi_k^2, \sigma_k^2\}$, $\forall k = 1, \ldots, q$, be the parameter vector. The joint posterior distribution of the parameters is expressed as

$$p(\theta|y) = \text{constant} \times p(y|\theta)p(\theta) \quad (8)$$

where

$$p(y|\theta) = \prod_{j=1}^{n} p(y_j|\beta, \gamma, \sigma^2) \quad (9)$$

is the likelihood and

$$p(\theta) = \prod_{k=1}^{q} p(\gamma_k|\alpha_k, \sigma_k^2)p(\alpha_k|\varphi_k^2)p(\sigma_k^2|\theta_\sigma)p(\varphi_k^2|\theta_\varphi) \quad (10)$$

is the prior distribution, where $\theta_\varphi = (\tau_\varphi, \omega_\varphi)$ and $\theta_\sigma = (\tau_\sigma, \omega_\sigma)$ for the scaled inverse Chi-square hyper-parameters, and $\theta_\varphi = \lambda_\varphi^2$ and $\theta_\sigma = \lambda_\sigma^2$ for the exponential hyper-parameters. The density (likelihood) for data y_j is

$$p(y_j|\beta, \gamma, \sigma^2) = N\left(y_j\middle|\beta + \sum_{k=1}^{q} Z_{jk}\gamma_k, \sigma^2\right) \quad (11)$$

The posterior mode estimates of all parameters are obtained by maximizing the log posterior distribution with any quantity involving γ_k and α_k replaced by the posterior expectation of that quantity.

EM algorithm

Derivation of the EM algorithm is straightforward and thus not provided in full length. In this section, we mainly focus on the EM steps by treating γ_k and α_k as missing values. We first give the expectation steps and then provide the maximization steps with brief derivation for some key elements.

Expectation steps

The expectation steps involve calculating the posterior expectations and posterior variances of missing values γ_k and α_k. The conditional posterior for the environment-specific QTL effect γ_k is normal with mean and variance specified below. The expectation is

$$E(\gamma_k|\cdots) = \left[\frac{1}{\sigma_k^2}I_{m\times m} + I_{m\times m}\sum_{j=1}^{n} Z_{jk}^2\right]^{-1}\left[\frac{1}{\sigma_k^2}1_m\alpha_k + \sum_{j=1}^{n} Z_{jk}y_j^*\right] \quad (12)$$

where

$$y_j^* = y_j - \beta - \sum_{k'\neq k}^{q} Z_{jk'}\gamma_{k'} \quad (13)$$

are the adjusted phenotypic values of line j by removing all other effects except the effects of locus k. The conditional posterior variance of γ_k is

$$\text{var}(\gamma_k|\cdots) = \left[\frac{1}{\sigma_k^2}I_{m\times m} + I_{m\times m}\sum_{j=1}^{n} Z_{jk}^2\right]^{-1} \quad (14)$$

The identity matrix $I_{m\times m}$ occurring in the above equation indicates that the expression is an $m \times m$ matrix, rather than a scalar. Similarly, the conditional posterior for α_k is normal with mean and variance given by

$$E(\alpha_k|\cdots) = \left[\frac{1}{\varphi_k^2} + \frac{m}{\sigma_k^2}\right]^{-1}\left[\frac{m}{\sigma_k^2}\sum_{t=1}^{m}\gamma_{jt}\right] \quad (15)$$

and

$$\text{var}(\alpha_k|\cdots) = \left[\frac{1}{\varphi_k^2} + \frac{m}{\sigma_k^2}\right]^{-1} \quad (16)$$

respectively. The conditional posterior means of γ_k and α_k are called the shrinkage estimates. Derivation of the shrinkage estimates can be found in Xu (2007).

Maximization steps

First, we describe the derivation for the posterior mode of σ_k^2. The target function for maximization is the expected complete-data log likelihood function. For the scaled inverse Chi-square prior, the part of the expected complete-data log likelihood function relevant to N_E is

$$L(\sigma_k^2|\tau_\sigma,\omega_\sigma) = -\frac{\tau_\sigma+2+m}{2}\ln(\sigma_k^2) - \frac{1}{2\sigma_k^2}\left\{\mathrm{E}\left[(\gamma_k-\alpha_k)^{\mathrm{T}}(\gamma_k-\alpha_k)\right]+\omega_\sigma\right\} \tag{17}$$

Setting $\frac{\partial}{\partial\sigma_k^2}L(\sigma_k^2|\tau_\sigma,\omega_\sigma)=0$ and solving for σ_k^2, we obtain

$$\sigma_k^2 = \frac{E\left[(\gamma_k-\alpha_k)^{\mathrm{T}}(\gamma_k-\alpha_k)\right]+\omega_\sigma}{\tau_\sigma+2+m} \tag{18}$$

where

$$E\left[(\gamma_k-\alpha_k)^{\mathrm{T}}(\gamma_k-\alpha_k)\right] = E(\gamma_k-\alpha_k)^{\mathrm{T}}E(\gamma_k-\alpha_k) + \mathrm{tr}[\mathrm{var}(\gamma_k|\cdots)] \tag{19}$$

and

$$E(\gamma_k-\alpha_k) = E(\gamma_k|\cdots) - E(\alpha_k|\cdots) \tag{20}$$

For the exponential (Lasso) prior, the part of the expected complete-data log likelihood function relevant to σ_k^2 is

$$L(\sigma_k^2|\lambda_\sigma) = -\frac{m}{2}\ln(\sigma_k^2) - \frac{E\left[(\gamma_k-\alpha_k)^{\mathrm{T}}(\gamma_k-\alpha_k)\right]}{2\sigma_k^2} - \frac{1}{2}\lambda_\sigma^2\sigma_k^2 \tag{21}$$

Setting $\frac{\partial}{\partial\sigma_k^2}L(\sigma_k^2|\lambda_\sigma)=0$ and solving for σ_k^2 leads to

$$\sigma_k^2 = \frac{\sqrt{m^2+4\lambda_\sigma^2 E\left[(\gamma_k-\alpha_k)^{\mathrm{T}}(\gamma_k-\alpha_k)\right]}-m}{2\lambda_\sigma^2} \tag{22}$$

The variance component φ_k^2 is derived using similar approach by maximizing the expected log posterior relevant to φ_k^2. Under the scaled inverse Chi-square prior, the final expression of the posterior mode is

$$\varphi_k^2 = \frac{E(\alpha_k^2)+\omega_\varphi}{\tau_\varphi+2+1} = \frac{E^2(\alpha_k|\cdots)+\mathrm{var}(\alpha_k|\cdots)+\omega_\varphi}{\tau_\varphi+2+1} \tag{23}$$

For the Lasso prior, we have two solutions with the positive one being

$$\varphi_k^2 = \frac{\sqrt{1+4\lambda_\varphi^2 E(\alpha_k^2)}-1}{2\lambda_\varphi^2} = \frac{\sqrt{1+4\lambda_\varphi^2[E^2(\alpha_k|\cdots)+\mathrm{var}(\alpha_k|\cdots)]}-1}{2\lambda_\varphi^2} \tag{24}$$

Given the updated random effects, let us deal with the fixed effect β and the residual error variance σ^2. The expected complete-data log posterior relevant to β and σ^2 is

$$L(\beta,\sigma^2) = -\frac{mn}{2}\ln\sigma^2 - \frac{1}{2\sigma^2}\sum_{j=1}^{n}E\left[(y_j-\beta-Z_j\gamma)^{\mathrm{T}}(y_j-\beta-Z_j\gamma)\right] \tag{25}$$

Setting $\frac{\partial}{\partial\beta}L(\beta,\sigma^2)=0$ and solving for β yields

$$\beta = \frac{1}{n}\sum_{j=1}^{n}\left[y_j - \sum_{k=1}^{q}Z_{jk}E(\gamma_k|\cdots)\right] \tag{26}$$

Finally, we set $\frac{\partial}{\partial\sigma^2}L(\beta,\sigma^2)=0$, solve for σ^2 and obtain the following solution

$$\sigma^2 = \frac{1}{mn}\sum_{j=1}^{n}E\left[(y_j-\beta-Z_j\gamma)^{\mathrm{T}}(y_j-\beta-Z_j\gamma)\right] \tag{27}$$

where the expectation of the quadratic form, denoted by $E(SS_j)$, has the following expression,

$$E(SS_j) = (y_j-\beta)^{\mathrm{T}}\left[y_j-\beta-\sum_{k=1}^{q}Z_{jk}(E\gamma_k|\cdots)\right] \tag{28}$$

The E-steps and M-steps are iterated repeatedly until a certain criterion of convergence is reached. At the final iteration, the estimated QTL effect for locus k is denoted by $\hat{\alpha}_k = E(\alpha_k|\cdots)$ and the corresponding variance for the estimate is $S_k^2 = \mathrm{var}(\alpha_k|\cdots)$. Similarly, the estimated environmental specific QTL effect vector is denoted by $\hat{\gamma}_k = E(\gamma_k|\cdots)$ and its variance–covariance matrix is denoted by $V_k = \mathrm{var}(\gamma_k|\cdots)$.

Hypothesis tests

There are two test statistics for each locus. The main effect QTL is tested under null hypothesis $H_0 : \alpha_k = 0$. The test statistic is the F-like statistics denoted by

$$F_k = \frac{\hat{\alpha}_k^2}{S_k^2} \tag{29}$$

The $Q \times E$ interaction effect for locus k is tested under null hypothesis $H_0 : \sigma_k^2 = 0$. Directly testing, this hypothesis is tedious because one has to reanalyze the data

under various reduced models. We reformulated the null hypothesis as $H_0 : \gamma_k = 1\alpha_k$, which is an alternative way of testing $\sigma_k^2 = 0$. The reason for this is that if all elements of vector γ_k are equal, we would expect that $\gamma_{k1} = \gamma_{k2} = \cdots = \gamma_{km} = \alpha_k$, and thus $Q \times E$ interaction is absent. We used the Wald statistic (Wald 1943) to test $Q \times E$ interaction,

$$W_k = (\hat{\gamma}_k - 1\hat{\alpha}_k)^{\mathrm{T}} V_k^{-1} (\hat{\gamma}_k - 1\hat{\alpha}_k) \tag{30}$$

Under the null model of $H_0 : \alpha_k = 0$, F_k will approximately follow an F-distribution with degrees of freedom 1 and n, where n is the sample size. When the sample size is sufficiently large, F_k will be approximated by a Chi-square distribution with one degree of freedom. Under the null model of $H_0 : \gamma_k = 1\alpha_k$ and assuming that n is relatively large, W_k will approximately follow a Chi-square distribution with m degrees of freedom. The critical values of these test statistics for significance declaration can be found from the percentiles of the corresponding central distributions. Alternatively, permutation tests (Churchill and Doerge 1994) may be used to draw empirical thresholds for the test statistics. In our data analysis, we used $\chi^2_{1,1-0.05} = 3.84$ as the critical value for testing the main QTL effect and $\chi^2_{m,1-0.05}$as the critical value for testing $Q \times E$ interaction. We discussed the reason why we did not use the permutation test in the final section of the manuscript.

Analysis of variances

Although the proportions of trait variance explained by each QTL and each $Q \times E$ interaction may be calculated using the sizes of estimated effects, it is very difficult to compute the overall contributions from all main effect QTL and from all $Q \times E$ interactions due to linkage of multiple QTL. We now use an analysis of variances (ANOVA) approach to partitioning the total phenotypic variance into variance due to all main effect QTL and variance due to all $Q \times E$ interactions. The ANOVA approach was suggested by one of the reviewers. The ANOVA can be accomplished with different analyses under three different models.

1. Full model:

The full model is described as

$$y_j = \beta + \sum_{k=1}^{q} Z_{jk}\gamma_k + \xi_j \tag{31}$$

where $\xi_j \sim N\left(0, I_{m\times m}\sigma_\xi^2\right)$ is the pure residual errors. Note that σ_ξ^2 is previously denoted by σ^2. This model facilitates an estimate of the environmental variance using the approach described early.

2. Main effect model:

The model assumes that there is no $Q \times E$ interaction and thus it can be formulated as

$$y_j = \beta + \sum_{k=1}^{q} Z_{jk} 1_m \alpha_k + \phi_j \tag{32}$$

where 1_m is an $m \times 1$ unity vector and $\phi_j \sim N\left(0, I_{m\times m}\sigma_\phi^2\right)$ is the residual error under the main effect model. Note that both Z_{jk} and α_k are scalars but the model is an $m \times 1$ vector, which explains why a unity vector is inserted there. This model facilitates an estimate of σ_ϕ^2.

3. Null model:

The null model assumes that there is neither QTL main effect nor $Q \times E$ interaction effect for the entire genome. The model only contains an intercept and a residual,

$$y_j = \beta + \zeta_j \tag{33}$$

where $\zeta_j \sim N\left(0, I_{m\times m}\sigma_\zeta^2\right)$ is the residual error under the null model.

We now have three models with three residual error variances. Under the three models, we obtain three estimated variances, $\hat{\sigma}_\xi^2$, $\hat{\sigma}_\varphi^2$ and $\hat{\sigma}_\zeta^2$. In terms of genetic variance components, the three residual variances are expected to be

$$\begin{aligned} E(\hat{\sigma}_\xi^2) &= \sigma_E^2 \\ E(\hat{\sigma}_\phi^2) &= \sigma_E^2 + \sigma_{Q\times E}^2 \\ E(\hat{\sigma}_\zeta^2) &= \sigma_E^2 + \sigma_{Q\times E}^2 + \sigma_Q^2 \end{aligned} \tag{34}$$

where σ_E^2 is the environmental variance, σ_Q^2 is the overall variance of main effects and $\sigma_{Q\times E}^2$ is the overall variance of $Q \times E$ interactions. Let $\sigma_P^2 = \sigma_E^2 + \sigma_{Q\times E}^2 + \sigma_Q^2$ be the total phenotypic variance. We are now able to estimate the proportions of phenotypic variance contributed by QTL main effects and $Q \times E$ interaction effects. The two proportions are

$$\hat{H}_Q = \frac{\hat{\sigma}_Q^2}{\hat{\sigma}_P^2} = \frac{\hat{\sigma}_\zeta^2 - \hat{\sigma}_\phi^2}{\hat{\sigma}_\zeta^2} \tag{35}$$

and

$$\hat{H}_{Q\times E} = \frac{\hat{\sigma}_{Q\times E}^2}{\hat{\sigma}_P^2} = \frac{\hat{\sigma}_\phi^2 - \hat{\sigma}_\xi^2}{\hat{\sigma}_\zeta^2} \tag{36}$$

Of course, we can report the so-called broad sense heritability using

$$\hat{H} = \hat{H}_Q + \hat{H}_{Q\times E} = \frac{\hat{\sigma}_Q^2 + \hat{\sigma}_{Q\times E}^2}{\hat{\sigma}_P^2} = \frac{\hat{\sigma}_\zeta^2 - \hat{\sigma}_\xi^2}{\hat{\sigma}_\zeta^2} \tag{37}$$

We have now concluded the methodology development.

Applications

Simulated data analysis

We simulated a single large chromosome of 1,120 cM in length covered by 225 codominant markers evenly spaced with 5 cM per marker interval. The simulated population contained $n = 150$ doubled diploid lines evaluated in 16 environments. The genotype indicator variable for line j at locus k was defined as $Z_{jk} = \{1, -1\}$, corresponding to the two genotypes A_1A_1 and A_2A_2. A total of 10 QTL were simulated with the sizes of the effects and genome locations given in Table 1 and depicted in Fig. 1 for the main effects and Fig. 2 for the $Q \times E$ interaction effects. The environmental error variance was set at $\sigma^2 = 50$. The simulation experiment was replicated 20 times and the average results were reported. In the analysis using the EM algorithm, we chose three different priors: (1) $(\tau, \omega) = (-2, 0)$ corresponding to the uniform prior (denoted by EM-Uniform), (2) $(\tau, \omega) = (0, 0)$ representing the Jeffrey's prior (denoted by EM-Jeffreys) and (3) the Lasso prior (denoted by EM-Lasso) with $\lambda_Q^2 = 1.9446$ and $\lambda_{Q\times E}^2 = 4.9852$. The Lasso parameters were estimated using the empirical formulas $\lambda_Q^2 = \left(\frac{1}{q}\sum_{k=1}^{q}\sigma_k^2\right)^{-\frac{1}{2}}$ for the main effects and $\lambda_{Q\times E}^2 = \left(\frac{1}{q}\sum_{k=1}^{q}\varphi_k^2\right)^{-\frac{1}{2}}$ for the $Q \times E$ interaction effects. The empirical method of choosing the Lasso parameter was proposed by Xu (2010). The same simulated data sets were also analyzed using the MCMC-implemented Bayesian method (Chen et al. 2010) for comparison. In the MCMC analysis, we used the uniform prior for the variance components, i.e., $(\tau, \omega) = (-2, 0)$. The length of the Markov chain contained 60,000 sweeps. The first 30,000 sweeps were deleted as they were considered as observations of the burn-in period. The Markov chain was then thinned at a rate of 1 out of 30. The empirical posterior sample contained 1,000 observations for the post-MCMC analysis. The MCMC experiment for each data analysis was repeated a few times using different seeds to make sure that the chains had converged to the stationary distributions. To test the significance of parameters of interest, we carried out a Bayesian permutation analysis proposed by Che and Xu (2010) to generate the null distributions of the QTL effects, from which an empirical threshold value was obtained for each QTL.

The true main effects and $Q \times E$ interaction effects along with their estimates are summarized in Table 1. Figure 1 depicts the true and estimated effects for QTL and Fig. 2 illustrates the true and estimated $Q \times E$ interaction effects. In terms of closeness of the estimated effects to the true effects, it appeared that the uniform prior of the EM algorithm (EM-Uniform) and MCMC algorithm (also using the uniform prior) produced better estimates than other methods while the MCMC algorithm was superior over the EM algorithm (EM-Uniform). In addition, the EM-Uniform and the MCMC algorithm are capable of separating closely linked QTL and detecting QTL only with main effects or only with $Q \times E$ interaction effects. For example, the second and third QTL had main effects in opposite directions and possessed no $Q \times E$ interaction effects. They were estimated very well by the two algorithms. The sixth QTL possessed $Q \times E$ interaction effect with no main effect. The seventh QTL had main effect only. Both the sixth and the seventh QTL were estimated well by the two algorithms. The Lasso prior produced estimated effects at the corresponding loci simulated, but the values were smaller than the true values, meaning strong shrinkage. The Jeffrey's prior had no power to detect the main effects, but was able to detect $Q \times E$ interaction effects. The failure of Jeffreys' prior for detecting the main effect QTL may be due to the strong shrinkage of the Jeffreys' prior compared to the uniform prior. Nevertheless, all algorithms provided accurate estimates for β and σ^2, which can be found in Table S1 of the Supplemental material.

To validate the analysis of variances for partitioning the total phenotypic variance into variance due to main effect QTL and variance due to $Q \times E$ interaction, we also simulated the data under various reduced models to determine the true H_Q and $H_{Q\times E}$. Although the genetic variances contributed by each QTL and $Q \times E$ interaction can be determined given the true effects, it is hard to determine the overall contributions due to linkage. Therefore, we used a simulation experiment to determine the overall contribution from each source. We simulated two extremely large populations with sample size 10,000 for each population. In the first population, the model was

$$g_j^{\text{full}} = \beta + \sum_{k=1}^{q} Z_{jk}\gamma_k \tag{38}$$

From this population, we calculated the variance of g_j^{full} across the 10,000 lines. This variance is $\text{var}\left(g_j^{\text{full}}\right) = \sigma_Q^2 + \sigma_{Q\times E}^2$. The second population was simulated under

$$g_j^{\text{main}} = \beta + \sum_{k=1}^{q} Z_{jk}\alpha_k \tag{39}$$

which provided $\text{var}\left(g_j^{\text{main}}\right) = \sigma_Q^2$. The difference between $\text{var}\left(g_j^{\text{full}}\right)$ and $\text{var}\left(g_j^{\text{main}}\right)$ gives the true value of $\sigma_{Q\times E}^2$. Once the true σ_Q^2, $\sigma_{Q\times E}^2$ and $\sigma_E^2 = 50$ were determined, we obtained σ_P^2, and thus were able to calculate the proportions of the trait variance contributed by the overall Q and $Q \times E$ interactions. The true proportions and their estimates from the analysis of variances are shown in Table 2.

Table 1 Simulated QTL main effects and $Q \times E$ interactions effects and their estimated values using the EM algorithms and the MCMC algorithm for 20 replicated simulation experiments

QTL ID (cM)	Main effect					$Q \times E$ interaction effects				
	True	EM-Uniform	EM-Jeffrey	EM-Lasso	MCMC	True	EM-Uniform	EM-Jeffrey	EM-Lasso	MCMC
1 (45)	3.1774	2.8345 (±0.2391)	0.0000 (±0.2882)	1.9382 (±0.2069)	3.1249 (±0.1440)	15.6341	14.4800 (±0.9766)	21.7345 (±1.0740)	7.7508 (±0.3434)	15.2919 (±1.0813)
2 (245)	−4.1395	−3.5875 (±0.5201)	0.0000 (±0.0000)	−1.9538 (±0.4592)	−3.6174 (±0.4185)	26.3211	24.9924 (±2.8046)	34.3821 (±2.7470)	10.9568 (±0.7419)	26.7689 (±2.9756)
3 (250)	2.6448	2.1867 (±0.4364)	0.0000 (±0.0000)	1.1357 (±0.3681)	2.2180 (±0.3549)	14.0425	12.0439 (±1.7527)	15.5249 (±2.2390)	6.3680 (±0.6926)	12.9048 (±1.7973)
4 (395)	3.1716	2.7745 (±0.4364)	0.0000 (±0.0000)	2.1647 (±0.3250)	3.0733 (±0.1350)	8.8099	8.4638 (±0.8013)	16.279 7 (±1.1059)	5.2522 (±0.3885)	9.0920 (±0.8335)
5 (495)	0.0000	0.0000 (±0.0003)	0.0000 (±0.0000)	−0.0001 (±0.0002)	−0.0365 (±0.1264)	7.7573	7.2245 (±0.6636)	5.7188 (±2.4093)	4.4099 (±0.3232)	7.2557 (±0.8025)
6 (645)	3.6336	3.4824 (±0.3061)	3.1525 (±0.1645)	2.5802 (±0.3141)	3.6894 (±0.2124)	11.4581	10.3164 (±1.1246)	9.4270 (±1.0923)	6.1990 (±0.5186)	10.6544 (±1.1599)
7 (745)	−3.0000	−2.6982 (±0.3006)	0.0000 (±0.0000)	−2.4783 (±0.3082)	−2.8449 (±0.1516)	0.0000	0.0192 (±0.0568)	7.7876 (±0.9004)	0.0134 (±0.0346)	0.3463 (±0.1424)
8 (895)	3.7301	3.3775 (±0.2882)	0.0000 (±0.0000)	2.6128 (±0.2110)	3.5734 (±0.1470)	11.5579	10.5296 (±1.1422)	20.9925 (±1.3359)	6.3348 (±0.3761)	11.1971 (±1.1081)
9 (995)	3.5485	2.8452 (±0.4602)	0.350603 (±0.7177)	2.7393 (±0.2395)	3.0400 (±0.6797)	6.7232	5.5139 (±2.5076)	14.4399 (±3.5960)	3.9694 (±1.2763)	6.6532 (±0.9380)
10 (1,095)	4.4746	4.2675 (±0.2728)	0.0000 (±0.0000)	3.1905 (±0.3288)	4.3109 (±0.2082)	15.3884	14.1816 (±1.3672)	29.5012 (±1.4246)	7.6920 (±0.5432)	15.1815 (±1.3665)

EM-Uniform: $(\tau, \omega) = (-2, 0)$; EM-Jeffrey: $(\tau, \omega) = (0, 0)$; EM-Lasso: $\lambda_Q^2 = 1.9446$ and $\lambda_{Q\times E}^2 = 4.9852$; MCMC-Bayesian method. The standard errors are included in the parentheses. The numbers in parentheses are standard deviations of the estimated effects across the 20 replicated experiments

We can see that the estimated H_Q and $H_{Q\times E}$ were very close to the true proportions.

Our simulation experiments showed that the EM algorithm with the uniform prior and the MCMC-implemented Bayesian method (uniform prior) are optimal in $Q \times E$ detection. The latter had a slight advantage over the former, but the advantage was barely noticeable. The great advantage of the EM algorithm is the fast computational speed. For each dataset, the EM algorithm required an average of 3.4 min of CPU time while the MCMC algorithm took 330.5 min on a desktop with an Inter Core i7-2600 3.4-GHz processor and 4.00 GB RAM (see the last row of Table 2). Therefore, the EM algorithm developed here can be a suitable alternative method for detecting $Q \times E$ interactions. The time consuming MCMC algorithm still has its advantages over the EM algorithm regarding the ability to generate an empirical posterior distribution (shape) for each estimated QTL effect while the EM algorithm only provides the posterior mode and posterior variance for each QTL.

Real data analysis

We applied the new EM algorithm to analyze the doubled-haploid population published by Hayes et al. (1993). The genotype and phenotype data were retrieved from the following two websites: http://www.genenetwork.org/genotypes/SXM.geno and http://wheat.pw.usda.gov/ggpages/SxM/phenotypes.html.

For the article to be self-contained, we briefly summarized the main features of the data. This dataset consisted of 150 doubled haploids (DH) derived from the cross of two spring barley varieties, Steptoe and Morex, designated as S × M. The traits consisted of three agronomic traits (Grain yield, Heading date and Height) and five malting quality traits (Lodging, Grain protein, Alpha amylase, Diastatic power and Malt extract). As an example, we only presented in detail the result of a malting quality trait named Lodging. This trait was measured in six environment and, therefore, $m = 6$ and $n = 150$. Other traits were also analyzed but results are not presented in detail as we did for Lodging (see Table 4 for all results). The total number of markers was 495 distributed along seven chromosomes of the barley genome. Because of the small sample size, we could not analyze all the 495 markers simultaneously in a single model due to high multi-collinearity. Therefore, we selected one marker in every 5 cM, leaving a total of 225 markers for the entire genome. If a selected genome location did not overlap with a marker, genotypes of the 150 lines were imputed from linked markers using the multipoint method (Jiang and Zeng 1997). The genotype of each marker was coded as +1 for the Steptoe allele and −1 for the Morex allele. All the 225

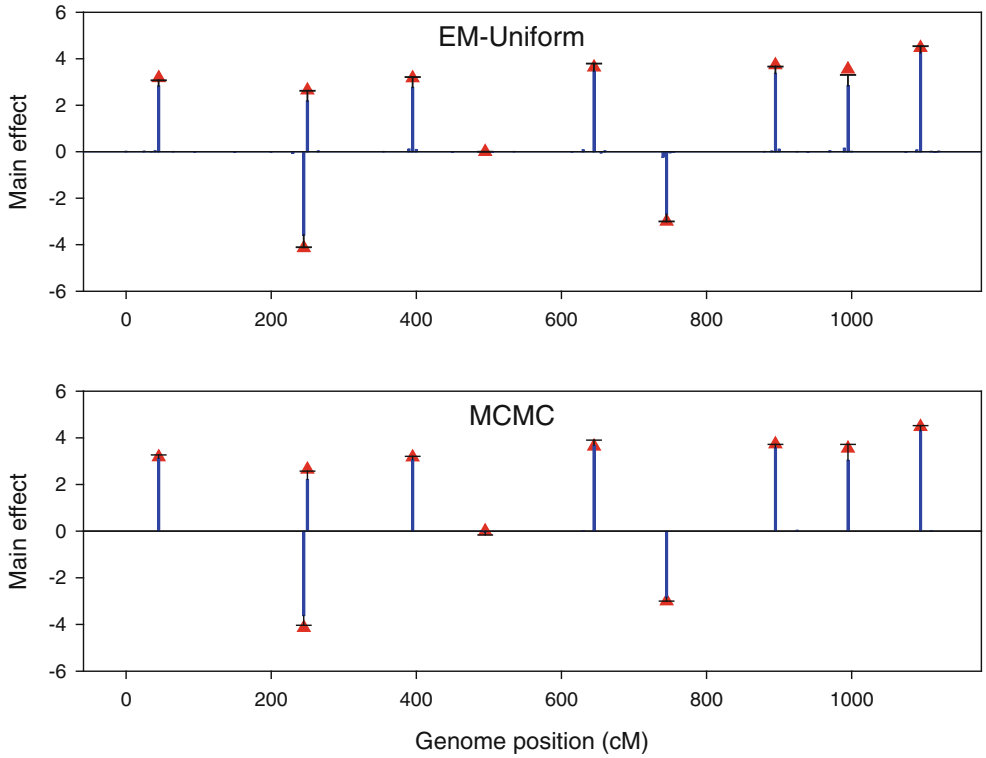

Fig. 1 True and estimated main effects of QTL plotted against genome location in the simulated data analysis. The red triangles indicate the true effects, the needles in blue show the estimated effects and error bars in black represent the standard errors. The top panel shows the result using the EM-Uniform algorithm and the bottom panel shows the result from the MCMC-implemented Bayesian method

putative loci were evaluated simultaneously in a single model.

We used the EM-Uniform algorithm and the MCMC algorithm to analyze this trait. The estimated QTL main effects are depicted in Fig. 3, where the top panel gives the result of the EM-Uniform and the bottom panel shows the result of the MCMC algorithm. The two methods generated similar results in most chromosome regions except a few places where the MCMC algorithm had extra peaks that were missing from the EM-Uniform algorithm. The major difference comes from the last chromosome where the EM-Uniform algorithm showed one peak but the MCMC algorithm gave two peaks (one overlaps with the one generated from the EM-Uniform algorithm). Another difference between the two methods is that the MCMC algorithm appears to have stronger shrinkage for large QTL but weaker shrinkage for smaller QTL than the EM-Uniform algorithm. The estimated $Q \times E$ interaction effects are depicted in Fig. 4, where the top panel shows the result of the EM-Uniform algorithm and the bottom panel shows that of the MCMC algorithm. Again, the two algorithms generated much the same result. The only difference is that the MCMC algorithm appeared to have spread each $Q \times E$ into a few smaller ones in the neighborhood of the major peak for some unknown reasons.

Result of analysis of variances for the trait Lodging is presented in Table 3. The two methods produced similar results regarding the estimated H_Q and $H_{Q\times E}$. On average, $\hat{H}_Q \approx 0.21$ and $\hat{H}_{Q\times E} \approx 0.31$ leading to an estimated broad sense heritability of $\hat{H} \approx 0.52$. The computational times for the EM-Uniform and MCMC algorithm were 5.20 and 289.05 min, respectively. Again, the advantage of the EM algorithm over the MCMC algorithm is well supported.

The F and W test statistics for the main effects and $Q \times E$ interaction effects for this trait (Lodging) are presented in Fig. 4. The critical value for main effect detection was $\chi^2_{1,0.95} = 3.84$ (one degree of freedom) and the corresponding critical value for $Q \times E$ detection was $\chi^2_{6,0.95} = 12.59$ (six degrees of freedom because there were six environments). Using these critical values, we detected $N_Q = 9$ main effect QTL and $N_{Q\times E} = 10$ interaction effects. Among these loci, $N_{Q\cap Q\times E} = 4$ of them showed both Q and $Q \times E$, and $N_{Q\cup Q\times E} = 9 + 10 - 4 = 15$ was the total number of loci with either Q or $Q \times E$ or both. Among the total number of loci detected, $N_Q/N_{Q\cup Q\times E} = 0.60$ had main effects and $N_{Q\times E}/N_{Q\cup Q\times E} = 0.67$ had $Q \times E$ interaction effects. Among the total number of loci evaluated ($N_{\text{Marker}} = 225$), $N_Q/N_{\text{Marker}} = 0.040$ had main effects and $N_{Q\times E}/N_{\text{Marker}} = 0.044$ had $Q \times E$ effects.

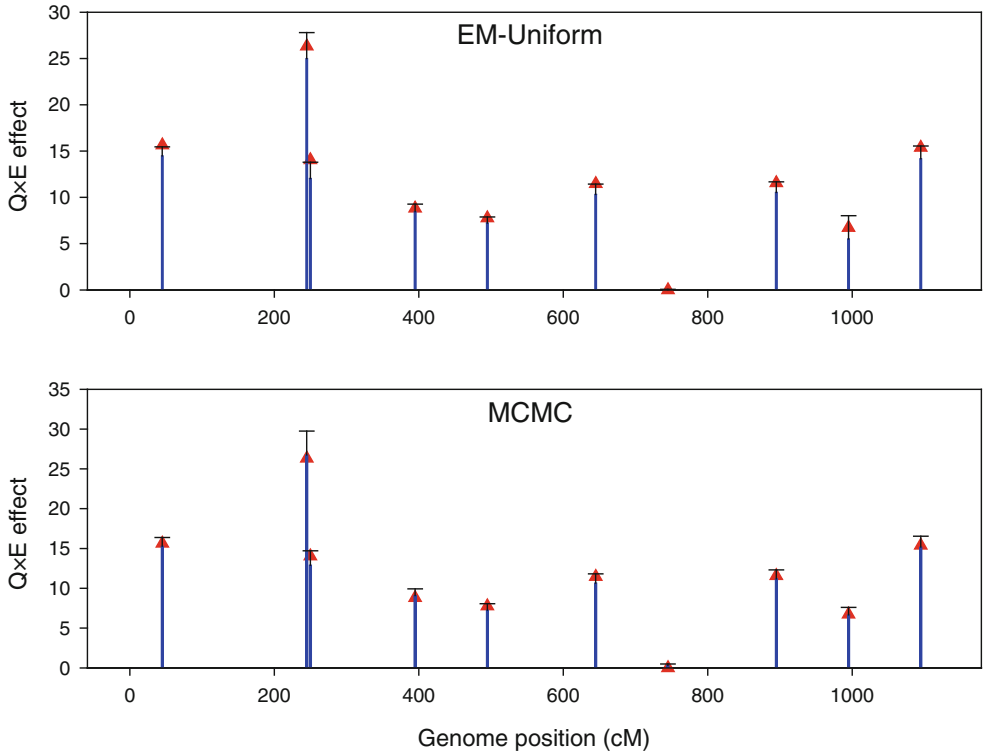

Fig. 2 True and estimated $Q \times E$ interaction effects plotted against genome location in the simulated data analysis. The red triangles indicate the true effects, the needles in blue show the estimated effects and error bars in black represent the standard errors. The top panel shows the result using the EM-Uniform algorithm and the bottom panel shows the result from the MCMC-implemented Bayesian method

Table 2 True and estimated proportions of phenotypic variance explained by QTL for the simulated data analysis

	True value	EM-Uniform	MCMC
Main (H_Q)	0.3546	0.3511 (±0.0064)	0.3534 (±0.0076)
$Q \times E$ ($H_{Q\times E}$)	0.4543	0.4682 (±0.0085)	0.4523 (±0.0090)
Computing time[a]	–	3.40 (±0.5000)	330.50 (±0.7631)

[a] The last row gives the computing time in minute for the two algorithms and the standard errors are included in parentheses

The overall proportion of the phenotypic variance contributed by main effects was $H_Q = 0.21$ and the corresponding proportion explained by $Q \times E$ was $H_{Q\times E} = 0.32$. Due to linkage, if two neighboring markers were both significant and in the same directions, we only counted as one. This would correct any upward bias regarding the estimated number of QTL. If a locus had a QTL effect but no $Q \times E$ interaction, but a locus 5 cM away from this locus showed $Q \times E$ interaction, we claimed that the Q and $Q \times E$ were in the same locus.

Finally, we used the EM-Uniform algorithm to analyze the remaining seven traits. Three of the seven traits were replicated in 16 environments and four of them were replicated in nine environments. The results of all trait analysis using the EM-Uniform algorithm (including Lodging measured in six environments) are summarized in Table 4. The number of QTL and $Q \times E$ interactions for the remaining seven traits was calculated using the same rules as we did for the Lodging analysis. For all the eight traits, on average, the proportion of trait variance explained by Q was $H_Q = 0.346$ and the corresponding proportion explained by $Q \times E$ was $H_{Q\times E} = 0.162$. The conclusion was that the main effect QTL played a more important role than the $Q \times E$ interaction effects. Another important discovery from Table 4 was that the number of loci showing both Q and $Q \times E$ was very small with an average of 2.75 across all eight traits. Majority of the loci showed either Q or $Q \times E$ but not both. Table 4 only provides a brief summary of the real data analysis. Detailed information regarding the actual estimated effects and locations of the significant loci are presented in Figures S1–S4 of the Supplemental material.

Discussion

We developed a hierarchical model for detection of $Q \times E$ interactions implemented via the EM algorithm. We also

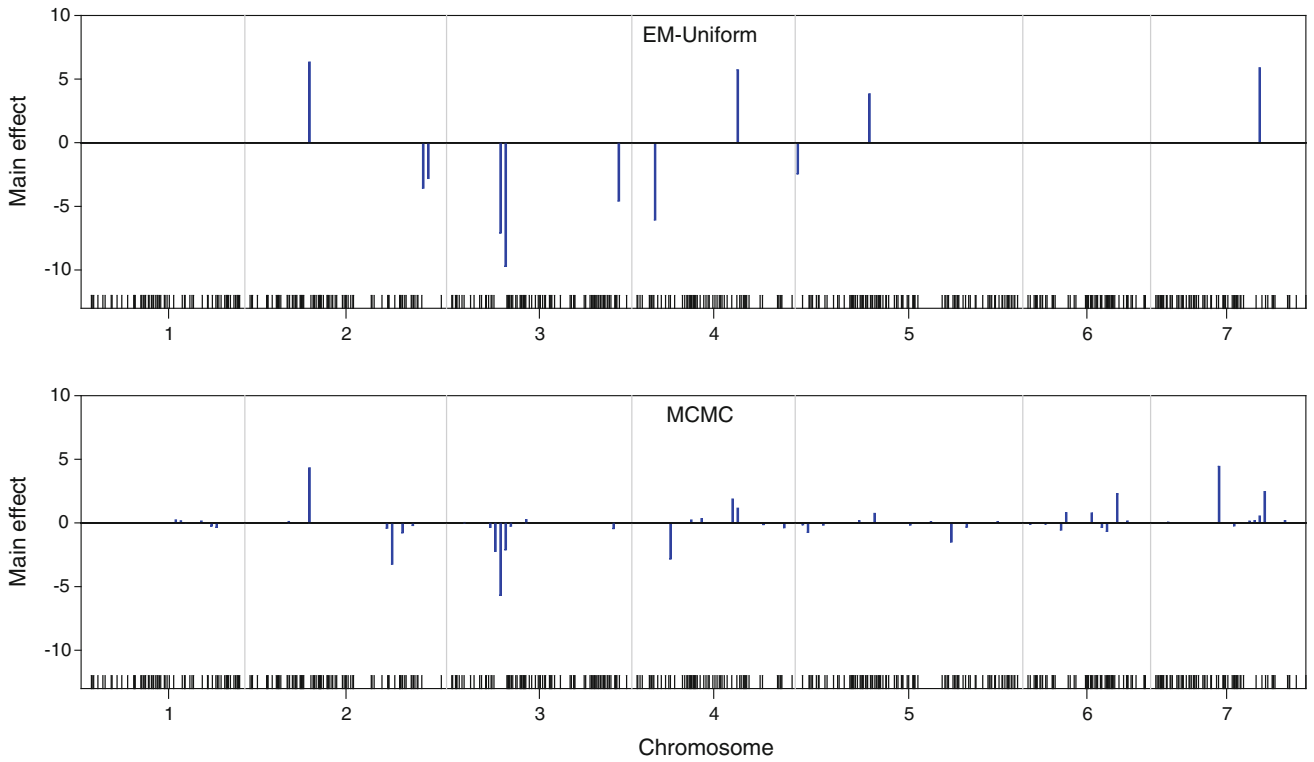

Fig. 3 Estimated main effects plotted against genome location for trait "Lodging" of the barley data analysis. The top panel shows the result of the EM-Uniform algorithm and the bottom panel shows the result of the MCMC algorithm. The seven chromosomes are separated by the vertical reference lines. The barcode like ticks on the *x*-axis represent the locations of the 495 markers

compared the EM algorithm with the Bayesian method (Chen et al. 2010) for detecting $Q \times E$ interactions. Results of the two methods are similar. The major advantage of the EM algorithm is the fast speed of computation. The Bayesian method, although slow in computation, still shows its advantage because it provides the posterior distribution (shape) for a QTL effect. This allows investigators to draw credibility interval for each estimated QTL effect. The EM algorithm, however, only gives the posterior mode and posterior variance for each QTL effect. Therefore, the EM algorithm is only a suitable alternative for the Bayesian method.

In the original data analysis of Hayes et al. (1993), the authors also reported $Q \times E$ interactions using the interval mapping approach (Haley and Knott 1992; Knapp et al. 1990) by analyzing the data separately with one environment at a time. They evaluated the differences of QTL effects among the environments. The original method is considered an ad hoc method. We examined the $Q \times E$ interaction effects detected from the ad hoc method and compared the results with ours. We found that all effects detected by Hayes et al. (1993) were also detected with our method. In addition, we detected more $Q \times E$ interaction effects (see Figures S1–S4 of the Supplemental material for the results of our analysis using the EM algorithm). This implied that our method may have higher power than the *ad hoc* method.

The hierarchical model presented is considered the simplest model of this kind. The reason is that we assumed $\xi_j \sim N(0, I_{m\times m}\sigma^2)$, which has the simplest residual variance structure. The simplest model seems to work well, as demonstrated in the barley data analysis. Further improvement may be done by incorporating more complicated residual variance structures. We did not do that in this study because (1) the result would be difficult to present and (2) it would be hard to partition the total variance into variance due to QTL main effects and variance due to $Q \times E$ interactions. In the future, we expect to see more experiments with traits measured in multiple environments. In any particular real data analysis, it is worthy to explore complicated error structures. The most advanced variance structure is the factor-analytic structure as given by Chen et al. (2010), in which the m environments are considered to be controlled by a few underlying factors. Extension of our model to factor-analytic structure is possible, although not a simple task. Two other structures are easy to incorporate, which are (1) the heterogeneous variance structure and (2) the fully unstructured variance matrix. The general covariance structure is $\xi_j \sim N(0, \Theta)$ where Θ is an $m \times m$ matrix. For the heterogeneous

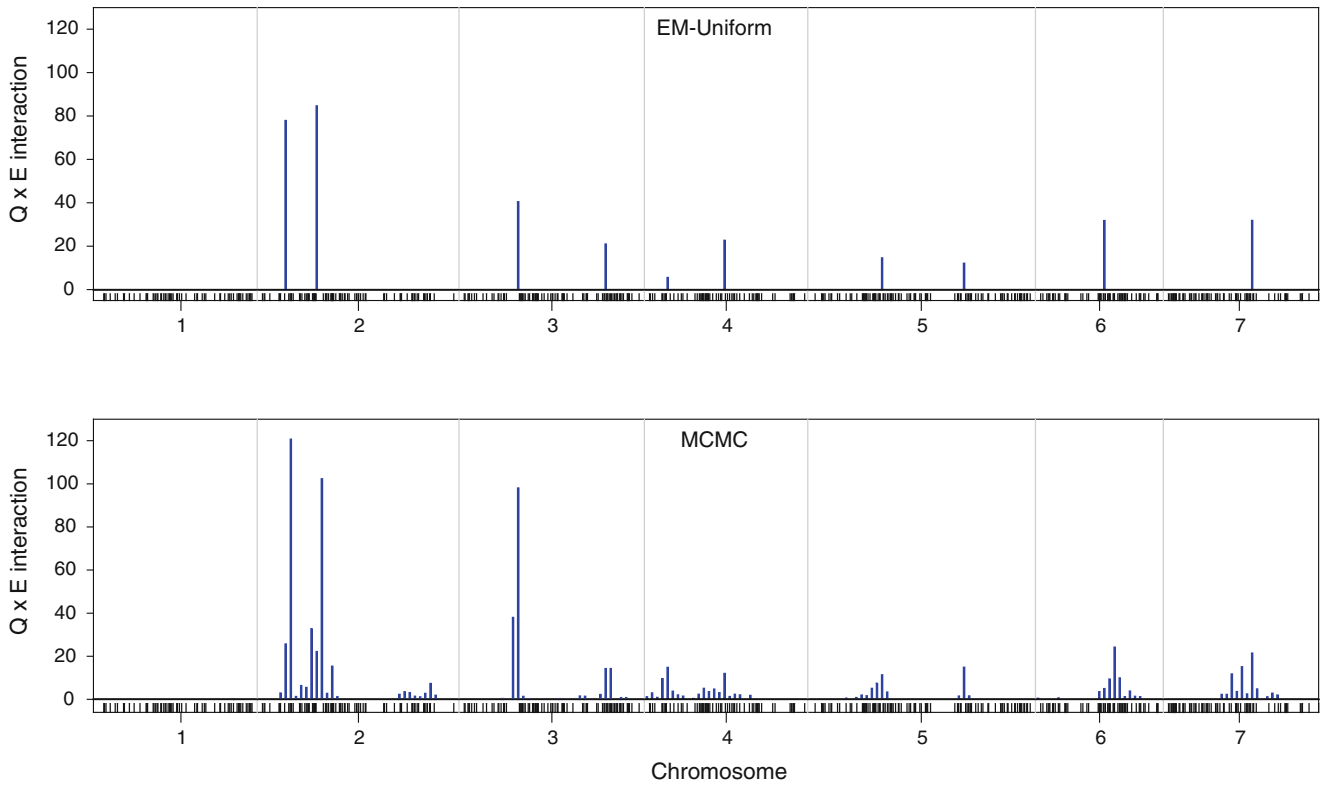

Fig. 4 Estimated $Q \times E$ interaction effects plotted against genome location for trait "Lodging" of the barley data analysis. The top panel shows the result of the EM-Uniform algorithm and the bottom panel shows the result of the MCMC algorithm. The seven chromosomes are separated by the vertical reference lines. The barcode like ticks on the x-axis represent the locations of the 495 markers

Table 3 Estimated proportions of phenotypic variance explained by QTL for trait Lodging of the barley data analysis

	EM-Uniform	MCMC
Main (H_Q)	0.2105	0.2297
$Q \times E$ ($H_{Q\times E}$)	0.3283	0.3071
Computing time[a]	5.20	289.05

[a] The last row gives the computing time in minute for the two algorithms

residual variance structure, $\Theta = D = \text{diag}\{d_1, \ldots, d_m\}$, where d_t is the variance for the tth environment. For the fully unstructured variance matrix, $\Theta = \Sigma$ is a positive definite symmetric matrix. To incorporate these variance structures, we need to replace $I_{m\times m}\sigma^2$ occurred in any place during the derivation of the simple structure by Θ. In addition, the maximization step for σ^2 is replaced by the maximization step for D using

$$D = \frac{1}{n}\sum_{j=1}^{n} \text{diag}\left\{E\left[\left(y_j - \beta - Z_j\gamma\right)\left(y_j - \beta - Z_j\gamma\right)^{\mathrm{T}}\right]\right\} \quad (40)$$

For the fully unstructured residual variance matrix, we need to replace the maximization step for σ^2 by the maximization step for Σ,

$$\Sigma = \frac{1}{n}\sum_{j=1}^{n} E\left[\left(y_j - \beta - Z_j\gamma\right)\left(y_j - \beta - Z_j\gamma\right)^{\mathrm{T}}\right] \quad (41)$$

Note that the transposition operator ($^{\mathrm{T}}$) occurs in the residual vector of the right, different from Eq. (27) in which $^{\mathrm{T}}$ occurred in the left. Chen et al. (2010) found that the D structure can have significant improvement over the simple structure, but the Σ structure may have only a marginal improvement. Again, we did not use D because we want to partition H into H_Q and $H_{Q\times E}$, which is not straightforward in situations other than the simple structure.

The hierarchical model involves hyper-parameters (τ, ω) for the scaled inverse Chi-square prior and λ^2 for the Lasso prior. For simplicity, we examined $(\tau, \omega) = (-2, 0)$ and $(\tau, \omega) = (0, 0)$ for the scaled inverse Chi-square prior. The Lasso prior λ^2 was drawn from the data using the empirical formula of Xu (2010). In real data analysis, these hyper-parameters may be determined by cross-validation analysis. The set of hype-parameters that generate the minimum squared prediction error (PE) should be selected and the results from that set of hyper-parameters should be reported.

Significance test is another issue in $Q \times E$ detection. We used the percentiles of central Chi-square distributions

Table 4 Summary statistics for eight quantitative traits in the "Steptoe" × "Morex" doubled-haploid barley population analysis using the EM-Uniform algorithm

	Trait								Average
	Yield	Lodging	Height	Heading	Grain protein	Alpha amylase	Diastatic power	Malt extract	
$N_{\text{Environment}}$	16	6	16	16	9	9	9	9	11.25
N_Q	18	9	39	32	15	22	26	11	21.50
$N_{Q\times E}$	9	10	3	2	3	6	10	5	6.00
$N_{Q\cap Q\times E}$	3	4	2	2	0	3	7	1	2.75
$N_{Q\cup Q\times E}$	24	15	40	32	18	25	29	15	24.75
$N_Q/N_{Q\cup Q\times E}$	0.7500	0.6000	0.9750	1.0000	0.8333	0.8800	0.8966	0.7333	0.8335
$N_{Q\times E}/N_{Q\cup Q\times E}$	0.3750	0.6667	0.0750	0.0625	0.1667	0.2400	0.3448	0.3333	0.0956
N_Q/N_{Marker}	0.0800	0.0400	0.1733	0.1422	0.0667	0.0978	0.1156	0.0489	0.0956
$N_{Q\times E}/N_{\text{Marker}}$	0.0400	0.0444	0.0133	0.0089	0.0133	0.0267	0.0444	0.0222	0.0267
$N_{Q\cap Q\times E}/N_{\text{Marker}}$	0.0133	0.0178	0.0089	0.0089	0.0000	0.0133	0.0311	0.0044	0.0122
H_Q	0.1145	0.2105	0.5208	0.6881	0.2335	0.3496	0.5620	0.0856	0.3456
$H_{Q\times E}$	0.3443	0.3283	0.1159	0.1212	0.0833	0.0915	0.1134	0.1006	0.1623

$N_{\text{Environment}}$, number of environments; N_{Marker}, number of markers; N_Q, number of main effects; $N_{Q\times E}$, number of $Q \times E$ interaction effects; $N_{Q\cup Q\times E}$, total number of effects (including Q and $Q \times E$); $N_{Q\cap Q\times E}$, number of loci showing both effects (Q and $Q \times E$ interaction effects); $N_Q/N_{Q\cup Q\times E}$, proportion of the number of main effect to total number of effects; $N_{Q\times E}/N_{Q\cup Q\times E}$, proportion of the number of $Q \times E$ interaction effects to the total number of effects; N_Q/N_{Marker}, proportion of the number of main effects to the total number of markers; $N_{Q\times E}/N_{\text{Marker}}$, proportion of the number of $Q \times E$ interaction effects to the total number of markers; $N_{Q\cap Q\times E}/N_{\text{Marker}}$, proportion of the number of effects to the total number of markers; H_Q, proportion of the trait variance contributed by overall main effects; $H_{Q\times E}$, proportion of the trait variance contributed by the overall $Q \times E$ interaction effects

as the critical values. Permutation tests (Churchill and Doerge 1994) may be used to generate empirical critical values. We hesitated using permutation tests because they were originally proposed for interval mapping. For multiple QTL analysis, its suitability is questionable. We believe that the multiple QTL mapping may have already considered the multiple tests, since the test for each marker is conditioned on all other markers. Anyway, the fact that we did not use permutation tests does not mean that other people should not use the permutation tests to draw the critical values. Assume that permutation tests can be justified for multiple QTL mapping, they can be easily implemented with the proposed EM algorithm because of the fast speed. The fact that our EM algorithm is developed based on the hierarchical model (a hybrid between Bayesian and frequentist approaches), the asymptotic theory derived based on the frequentist approach may not apply to the hierarchical model. As a result, the test statistics may not follow the corresponding central distributions under the null models. Therefore, the permutation test for drawing the critical values of the test statistics may be an alternative way to decide the significance of a detected QTL effect. Permutation tests for multiple QTL mapping should be thoroughly investigated before they can be comfortably applied to this kind of multiple QTL models.

From genomic selection point of view, significance tests may not be required because all markers should be applied to predict the whole genome effect for each line, regardless how small their effects are (Meuwissen et al. 2001). Recently, genomic selection has become a hot topic for animal and plant breeding (Goddard and Hayes 2007, 2009; Goddard et al. 2010; Hayes et al. 2009; Heffner et al. 2009; Jannink et al. 2010; Meuwissen et al. 2001; Nielsen et al. 2009; Schaeffer 2006; Sonesson and Meuwissen 2009; Xu 2003; Xu and Hu 2010; Zhang et al. 2011). Genomic selection using multiple environmental data should be a useful subject for further investigation.

Acknowledgments We greatly appreciate two anonymous reviewers and the associated editor for their comments on an early version of the manuscript and their suggestions in revision of the manuscript. The project was supported by the USDA National Institute of Food and Agriculture Grant 2007-02784 to SX.

References

Attari HE, Hayes P, Rebai A, Barrault G, Dechamp-Guillaume G, Sarrafi A (1998) Potential of doubled-haploid lines and localization of quantitative trait loci (QTL) for partial resistance to bacterial leaf streak (Xanthomonas campestris pv. hordei) in barley. TAG Theor Appli Genet 96:95–100

Che X, Xu S (2010) Significance test and genome selection in bayesian shrinkage analysis. Int J Plant Genomics. doi:10.11155/2010/893206

Chen X, Zhao F, Xu S (2010) Mapping environment-specific quantitative trait loci. Genetics 186:1053–1066

Churchill GA, Doerge RW (1994) Empirical threshold values for quantitative trait mapping. Genetics 138:963–971

Fang M, Jiang D, Pu LJ, Gao HJ, Ji P, Wang HY, Yang RQ (2008) Multitrait analysis of quantitative trait loci using Bayesian composite space approach. BMC Genet 9:48. doi:10.1186/1471-2156-9-48

Goddard M, Hayes B (2007) Genomic selection. J Anim Breed Genet 124:323–330

Goddard M, Hayes B (2009) Mapping genes for complex traits in domestic animals and their use in breeding programmes. Nat Rev Genet 10:381–391

Goddard M, Hayes B, Meuwissen T (2010) Genomic selection in livestock populations. Genetics Res 92:413–441

Haley C, Knott S (1992) A simple regression method for mapping quantitative trait loci in line crosses using flanking markers. Heredity 69:315–324

Han F, Ullrich S, Chiarat S, Menteur S, Jestin L, Sarrafi A, Hayes P, Jones B, Blake T, Wesenberg D, Kleinhofs A, Kilian A (1995) Mapping of beta glucan content and beta glucanase activity loci in barley grain and malt. Theor Appl Genet 91:921–927

Han F, Ullrich S, Kleinhofs A, Jones B, Hayes P, Wesenberg D (1997) Fine structure mapping of the barley chromosome-1 centromere region containing malting-quality QTLs. TAG Theor Appl Genet 95:903–910

Hayes P, Liu B, Knapp S, Chen F, Jones B, Blake T, Franckowiak J, Rasmusson D, Sorrells M, Ullrich S (1993) Quantitative trait locus effects and environmental interaction in a sample of North American barley germ plasm. Theor Appl Genet 87:392–401

Hayes B, Bowman P, Chamberlain A, Goddard M (2009) Genomic selection in dairy cattle: progress and challenges. J Dairy Sci 92:433–443

Heffner EL, Sorrells ME, Jannink JL (2009) Genomic selection for crop improvement. Crop Sci 49:1–12

Henderson C (1975) Best linear unbiased estimation and prediction under a selection model. Biometrics 31(2):423–447

Jannink JL, Lorenz AJ, Iwata H (2010) Genomic selection in plant breeding: from theory to practice. Brief Funct Genomics 9:166–177

Jiang C, Zeng ZB (1997) Mapping quantitative trait loci with dominant and missing markers in various crosses from two inbred lines. Genetica 101:47–58

Knapp S, Bridges W, Birkes D (1990) Mapping quantitative trait loci using molecular marker linkage maps. Theor Appl Genet 79:583–592

Meuwissen T, Hayes B, Goddard M (2001) Prediction of total genetic value using genome-wide dense marker maps. Genetics 157:1819–1829

Nielsen HM, Sonesson AK, Yazdi H, Meuwissen THE (2009) Comparison of accuracy of genome-wide and BLUP breeding value estimates in sib based aquaculture breeding schemes. Aquaculture 289:259–264

Piepho HP (2000) A mixed-model approach to mapping quantitative trait loci in barley on the basis of multiple environment data. Genetics 156:2043–2050

Romagosa I, Ullrich SE, Han F, Hayes PM (1996) Use of the additive main effects and multiplicative interaction model in QTL mapping for adaptation in barley. TAG Theor Appl Genet 93:30–37

Schaeffer L (2006) Strategy for applying genome wide selection in dairy cattle. J Anim Breed Genet 123:218–223

Sonesson AK, Meuwissen THE (2009) Testing strategies for genomic selection in aquaculture breeding programs. Genet Sel Evol 41:37

Tibshirani R (1996) Regression shrinkage and selection via the lasso. J Roy Stat Soc Ser B 58(1):267–288

Wald A (1943) Tests of statistical hypotheses concerning several parameters when the number of observations is large. Trans Am Math Soc 54:426–482

Xu S (2003) Estimating polygenic effects using markers of the entire genome. Genetics 163:789–801

Xu S (2007) Derivation of the shrinkage estimates of quantitative trait locus effects. Genetics 177:1255–1259

Xu S (2010) An expectation–maximization algorithm for the Lasso estimation of quantitative trait locus effects. Heredity 105:483–494

Xu S, Hu Z (2010) Methods of plant breeding in the genome era. Genet Res 92:423–441

Yi N, Xu S (2008) Bayesian LASSO for quantitative trait loci mapping. Genetics 179:1045–1055

Zhang Z, Zhang Q, Ding X (2011) Advances in genomic selection in domestic animals. Chin Sci Bull 56:2655–2663